ISBN: 978-3-95450-223-3 ISSN: 2673-7000 doi:10.18429/JACoW-NAPAC2019-MOPLH19

BEAM DYNAMICS SIMULATIONS FOR A CONDUCTION-COOLED SUPERCONDUCTING RF ELECTRON SOURCE *

O. Mohsen†, V. Korampally, A. McKeown, D. Mihalcea, P. Piot‡, I. Salehinia
Northern Illinois University, DeKalb, IL, USA
R. Dhuley, M.G. Geelhoed, J.C.T. Thangaraj
Fermi National Accelerator Laboratory, Batavia, IL, USA

Abstract

The development of robust and portable high-average power electron sources is key to many societal applications. An approach toward such sources is the use of cryogen-free superconducting radiofrequency cavities. This paper presents beam-dynamics simulations for a proof-of-principle experiment on a cryogen-free SRF electron source being prototyped at Fermilab [1]. The proposed design implement a geometry that enhances the electric field at the cathode surface to simultaneously extract and accelerate electrons. In this paper, we explore the beam dynamics considering both the case of field and photoemission mechanism.

INTRODUCTION

Electron accelerators are finding a great interest in many scientific [2,3], industrial and societal applications [4]. Their advancement relies heavily on the development of electron sources and the coupled accelerating structures. Some of the contemplated applications call for low-cost, rugged, and portable electron accelerators capable of producing high-average-power beams. Recent advances in photo-injectors, specifically, the coupling between photoemission sources and Superconducting radio-frequency (SRF) technologies enabled the generation of very high peak current and low emittance beams [2,5]. So far, this required the operation of an auxiliary laser system which usually increases the cost and the complexity of the accelerator. Moreover, current laser systems can generate high power pulses on a moderate repetition rate [$\mathcal{O}$(kHz)], which ultimately limits the average current. On the contrary, field emission (FE) enables the emission of electrons from the bulk of a material subjected to intense electric fields [6]. Thus, an FE source does not require the additional triggering by a laser system. Likewise, when integrated into an RF structure, the emission from the FE cathode is self gated by and synchronized with, the RF electric field. Such a feature enables the extraction of electrons in every RF cycle, which pave the way to the production of high-average-power beams [7,8].

* This work was supported by the US Department of Energy (US DOE) under award No. DE-SC0018367 with Northern Illinois University. Fermilab is managed by the Fermi Research Alliance, LLC under US DOE contract No. DE-AC02-07CH11359. This research used resources of the National Energy Research Scientific Computing Center which is supported by the US DOE contract No. DE-AC02-05CH11231.
† omohsen@niu.edu
‡ also at Fermi National Accelerator Laboratory, Batavia, IL, USA

In this paper, we perform numerical simulations of a proposed superconducting RF (SRF) FE electron source experiment in preparation at Fermilab [1]. This concept experiment will investigate FE cathodes operation in SRF cavities. However, the source can in principle also operate with photoemission cathodes and the corresponding beam dynamics is also explored.

CONCEPTUAL DESIGN: OVERVIEW

The initial design of the proposed electron source is based on a niobium 650 MHz single-cell elliptical resonator with the geometry shown in Fig. 1(a) [1]. The resonator is flanked with 50 mm beam pipes with flanges on each side. In order to support experiment on electron emission, the resonator was modified by inserting a stud of length $L = 0.22$ m and radius $r = 5$ mm; see Fig. 1(b). The addition of the stud modifies the resonant modes inside the resonator, thus changing the electromagnetic field distribution inside the resonator. The altered configuration enables the field at the stud extremity where the cathode is located to be maximum. To avoid significant field enhancement at the edge of the rod, its tip is rounded with a fillet with 1-mm radius of curvature. The dimensions of the rod and the radius of curvature of

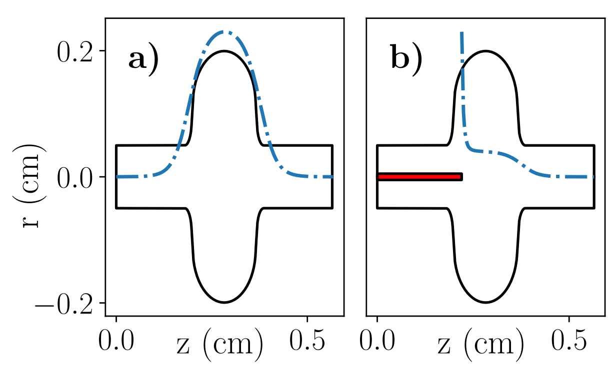

Figure 1: Geometry of the nominal (a) and modified cavity (b). The blue dashed lines corresponds to the on-axis electric field $Ez(z, r = 0)$.

the fillet were determined in a previous study based on the electromagnetic and thermal simulations available experimental equipment [1]. Thermal consideration prevented us to maximize the field by locating the rod extremity exactly at the center of the cell (instead it had to be slightly retracted). Both end flanges at $z = 0.0$ m and $z \sim 0.56$ m (input and

Content from this work may be used under the terms of the CC BY 3.0 licence (© 2019). Any distribution of this work must maintain attribution to the author(s), title of the work, publisher, and DOI

ISBN: 978-3-95450-223-3 ISSN: 2673-7000 doi:10.18429/JACoW-NAPAC2019-MOPLH19

Content from this work may be used under the terms of the CC BY 3.0 licence (© 2019). Any distribution of this work must maintain attribution to the author(s), title of the work, publisher, and DOI

pickup flange, respectively) will host auxiliary instrumentation for supplying the RF power and beam diagnostics. The electron-beam diagnostics consists of Faraday cup made of a 40 mm-radius copper disk.

A key aspect of this design is the use of direct heat conduction to achieve cryogenic temperatures using a cryocooler (Cryomech PT420). Such cryogen-free high-current electron sources have a lower operating cost, a smaller footprint, and has a higher likelihood to be deployed in, e.g., industrial environment [9, 10] compared to conventional SRF sources which necessitate liquid helium.

BEAM DYNAMICS SIMULATION

Field Emission Study

Beam physics studies of the electrons extracted at the stud tip via FE were performed using the particle-in-cell (PIC) program WARP [11] which includes an FE model. In the simulation, the cathode was considered to be a circular surface of a 2-mm radius and located at the extremity of the stud (at $z = 22$ cm). The electromagnetic fields were simulated using omega3p [12] and imported to WARP. The

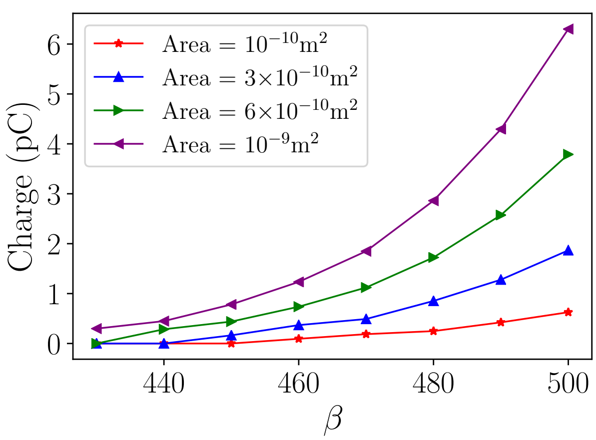

Figure 2: Charge extracted downstream the electron source for different field enhancement factor β and different effective emission area A_e. The applied electric field is E_0 = 8.6 MV/m.

cathode radius was chosen to be much smaller than the tip radius (5 mm) to achieve a uniform emission across the cathode and to prevent excessive transverse field. In the simulation, the macroparticles are generated at each grid point on cathode surface according to Fowler-Nordheim distribution evaluated with the local electric field value and the field emission parameters; i.e field enhancement β and emission effective area A_e. The field emission parameters were chosen to match FE cathodes experimentally study by our group [13]. The field-emitted particles are then pushed through the electromagnetic field of the resonator from the cathode to the pickup flange. The value of the peak field at the cathode is determined by the power capacity of the cryocooler and input power of the low-level RF system (LLRF) and was estimated to $E_0 \simeq 8.6\,\mathrm{MV\,m^{-1}}$). Figure 2

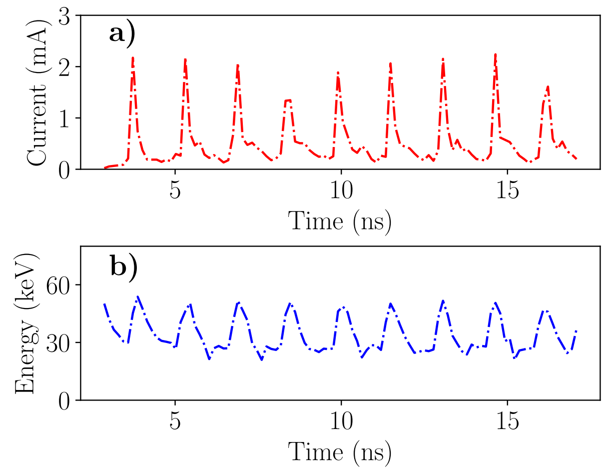

Figure 3: Electron beam current (a) and the average kinetic energy (b) downstream of the electron source.

shows the charge extracted from the cathode within one RF bucket and transmitted up to the downstream flange as a function of the enhancement factor. Beam current and mean energy downstream the gun is shown in Fig. 3. The bunch peak current $I \simeq 2$ mA with a corresponding kinetic energy of the beam $K > 50$ keV.

Photo Emission Study

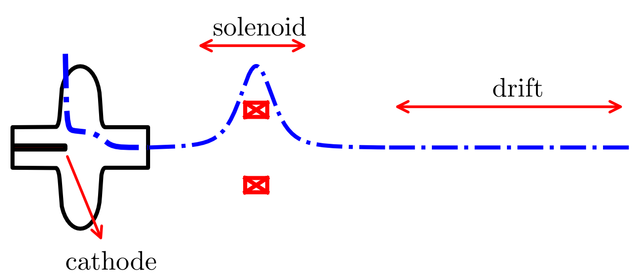

Figure 4: Envisioned beamline for photo-emission applications. The distance between the cathode to the center of the solenoid and the length of the drift were determined via optimization; i.e see Table 1.

In the absence of nonlinear and collective effects, the emitted electron distribution from the photocathode represents the initial laser pulse. In the present work, we consider the use of a solenoid to compensate for the space-charge-driven emittance growth; see Fig. 4. The beam dynamics simulations were carried out using impact-t, a PIC beam-dynamics code [14]. To minimize the emittance downstream the beamline, we use the package deap, a python based optimization framework. In the optimization, the laser spot size and emission time, as well as the lunch phase, solenoid strength, and length of the drift were variables and determined in the optimization. We use the optimized laser parameters to generate a particle distribution that is pushed in IMPACT-T through the proposed beamline. Table 1 summarizes the optimization parameters and output. In the simulation, a moderate beam charge was used (Q = 500 fC). Fig 5 shows the evo-

ISBN: 978-3-95450-223-3 ISSN: 2673-7000 doi:10.18429/JACoW-NAPAC2019-MOPLH19

Table 1: Beam Line Settings and Simulated Beam Parameters Downstream of the Envisioned Beam Line

Parameter	**value**	**unit**
number of macro particles	200,000	-
emission time (rms)	4.6	ps
laser spot size	0.53	mm
lunch phase	91.45	deg
drift length	3.87	m
solenoid strength	7.4	mT
final beam energy	116.0	keV
Final transverse emittance (rms)	26	nm rad
final bunch duration (rms)	21.0	ps

lution of the transverse RMS emittance ϵ_x and the beam size σ_r through the beamline. Both the emittance (RMS) and beam size (RMS) reach final values of ~ 25 nm rad and 0.13 mm, respectively. Figure 6 shows snapshots of the transverse and longitudinal phase spaces along the beamline. The bunch duration downstream the beamline is $\sigma_t \sim 21$ ps and the final energy of the beam $E \sim 115$ keV; see Table 1.

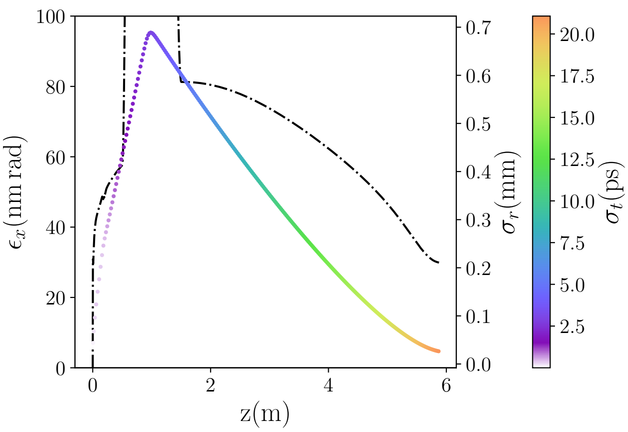

Figure 5: Simulation results of the rms emittance (dashed black) and rms beam size (dotted). The colors in dotted line represent the bunch duration in ps.

CONCLUSION & FUTURE WORK

In summary, we presented initial simulations for the previously described electron source. The simulations covered beam dynamics for the case of field emission and photoemission cathodes. The proposed gun will be mainly used for field emission applications. When compared with field emission parameters tested earlier, the current produced downstream the gun is detectable and in the range of mA. So far, the output beam in the case of the field emission study is not optimized. However, the possible use of a focusing solenoid just in case of the photoemission case is still possible. For the case of photoemission, the early-stage simulation suggests that moderate to low transverse emittance could be generated provided that a laser system is available. The small size of the setup and the use of the cryocooler makes this design ideal for use outside scientific laboratories.

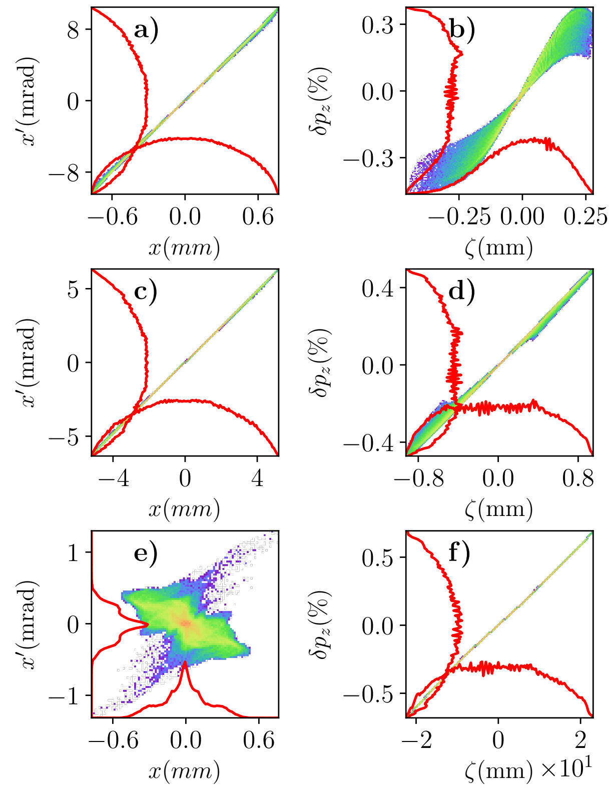

Figure 6: Transverse trace-space (a,c,d) and longitudinal phase-space (b,d,f) recorded after the cathode z= 1cm (a,b), after the gun z= 34 cm (c,d) and at downstream the beamline z= 550 cm.

Further work on reducing the bunch duration to fs scales and increasing the energy, possibly by considering multiple cell resonator is also possible.

On the experimental front, the part to implement the modified cavity geometry of Fig. 1(b) has been completed along with the thermal links necessary to improve the cavity cooling. As a first stage, frequency analysis will be done without cooling down the resonator. Soon afterward, the cavity will be cooled down and thermal and electromagnetic analysis will be done. Finally, an FE cathode will be attached to the stud and the extracted current will be measured. A second phase of the project will involve a cryostat proper thermal transition to allow for transport of the electron bunches in a downstream beamline.

ACKNOWLEDGEMENTS

The authors would like to thank Cho-Kuen Ng and Liling Xiao from SLAC for their useful tips and comments on using OMEGA3P.

REFERENCES

[1] O. Mohsen, R. Dhuley, M. Geelhoed, A. McKeown, D. Mihalcea, P. Piot, I. Salehinia, and J. Thangaraj, “Simulations and experimental plans for a high-repetition-rate field-enhanced conduction-cooled superconducting rf electron source,” in

Content from this work may be used under the terms of the CC BY 3.0 licence (© 2019). Any distribution of this work must maintain attribution to the author(s), title of the work, publisher, and DOI

ISBN: 978-3-95450-223-3 ISSN: 2673-7000 doi:10.18429/JACoW-NAPAC2019-MOPLH19

Content from this work may be used under the terms of the CC BY 3.0 licence (© 2019). Any distribution of this work must maintain attribution to the author(s), title of the work, publisher, and DOI

10th Int. Particle Accelerator Conf.(IPAC'19), pp. 2113–2116, Melbourne, Australia, May 2019.

[2] Y. Ding, A. Brachmann, F.-J. Decker, D. Dowell, P. Emma, J. Frisch, S. Gilevich, G. Hays, P. Hering, Z. Huang *et al.*, "Measurements and simulations of ultralow emittance and ultrashort electron beams in the linac coherent light source," *Phys. Rev. Lett.*, vol. 102, no. 25, p. 254801, 2009.

[3] S. Weathersby, G. Brown, M. Centurion, T. Chase, R. Coffee, J. Corbett, J. Eichner, J. Frisch, A. Fry, M. Gühr, *et al.*, "Mega-electron-volt ultrafast electron diffraction at slac national accelerator laboratory," *Rev. Sci. Instrum.*, vol. 86, no. 7, p. 073702, 2015.

[4] R. Kephart *et al.*, "SRF compact accelerators for industry and society," in *Proc. SRF2015*, pp. 1467–1469, Whistler, BC, Canada, Sep. 2015.

[5] J. Maxson, D. Cesar, G. Calmasini, A. Ody, P. Musumeci, and D. Alesini, "Direct measurement of sub-10 fs relativistic electron beams with ultralow emittance," *Phys. Rev. Lett.*, vol. 118, no. 15, p. 154802, 2017.

[6] R. H. Fowler and L. Nordheim, "Electron emission in intense electric fields," in *Proc. of the Royal Society of London A*, vol. 119, pp. 173–181, The Royal Society, 1928.

[7] J. Lewellen and J. Noonan, "Field-emission cathode gating for rf electron guns," *Phys. Rev. Spec. Top. Accel Beams*, vol. 8, no. 3, p. 033502, 2005.

[8] O. Mohsen, I. Gonin, R. Kephart, T. Khabiboulline, P. Piot, N. Solyak, J. Thangaraj, and V. Yakovlev, "Initial beam dynamics simulations of a high-average-current field-emission electron source in a superconducting radiofrequency gun," *Nucl. Instrum. Methods Phys. Res., Sect. A*, vol. 909, pp. 456–459, 2018.

[9] R. Dhuley, R. Kostin, O. Prokofiev, M. Geelhoed, T. H. Nicol, S. Posen, J. C. T. Thangaraj, T. Kroc, and R. Kephart, "Thermal link design for conduction cooling of srf cavities using cryocoolers," *IEEE Trans. Appl. Supercond.*, vol. 25, p. 0500205, 2019.

[10] R. Dhuley, M. Geelhoed, and J. Thangaraj, "Thermal resistance of pressed contacts of aluminum and niobium at liquid helium temperatures," *Cryogenics*, vol. 93, pp. 86–93, 2018.

[11] A. Friedman, R. H. Cohen, D. P. Grote, S. M. Lund, W. M. Sharp, J.-L. Vay, I. Haber, and R. A. Kishek, "Computational methods in the warp code framework for kinetic simulations of particle beams and plasmas," *IEEE Transactions on Plasma Science*, vol. 42, no. 5, pp. 1321–1334, 2014.

[12] L.-Q. Lee, Z. Li, C. Ng, K. Ko, *et al.*, "Omega3p: A parallel finite-element eigenmode analysis code for accelerator cavities," tech. rep., Stanford Linear Accelerator Center (SLAC), 2009.

[13] O. Mohsen, R. Divan, V. Korampally, A. Lueangaramwong, P. Piot, A. Sumant, and S. Valluri, "Performances of silicon-based field-emission cathodes coated with ultranano crystalline diamond," in *10th Int. Particle Accelerator Conf. (IPAC'19)*, pp. 2117–2120, Melbourne, Australia, May 2019.

[14] J. Qiang, S. Lidia, R. D. Ryne, and C. Limborg-Deprey, "Three-dimensional quasistatic model for high brightness beam dynamics simulation," *Phys. Rev. Spec. Top. Accel Beams*, vol. 9, no. 4, p. 044204, 2006.